LAWRENCE
LIVERMORE
NATIONAL
LABORATORY

LLNL-JRNL-822768

ICP Etching of GaN Microstructures in a Cl2-Ar Plasma with Subnanometer-scale Sidewall Surface Roughness

C. D. Frye, C. E. Reinhardt, S. B. Donald, L. F. Voss, S. E. Harrison

May 19, 2021

Materials Science in Semiconductor Processing

Disclaimer

ICP etching of GaN microstructures in a Cl_2-Ar plasma with subnanometer-scale sidewall surface roughness

Keywords: Gallium Nitride, Plasma Etching, Surface Roughness, Wide Bandgap

Clint D. Frye,[1,a)] Catherine E. Reinhardt,[1] Scott B. Donald,[1] Lars F. Voss, [1] and Sara E. Harrison[1]

[1] Lawrence Livermore National Laboratory, 7000 East Avenue, Livermore, CA 94550

[a)] Electronic mail: frye6@llnl.gov

Substrate temperature, RF power, and ICP power were investigated for their effects on GaN micropillar sidewall roughness and etch characteristics. Elevated substrate temperature was shown to improve the sidewall etch morphology at low RF powers (reduced physical bombardment) and low ICP powers (lower plasma densities). Increased lateral etching is observed with both increased ICP power and substrate temperature, which both act to increase the chemical component of the etch. Etch conditions with a high chemical driving force resulted in faceting along the a-plane on the sidewalls. This faceting produced extremely smooth surfaces with root-mean-square roughness (R_q) as low as 0.20 nm which is comparable to typical epitaxy-ready surfaces and smaller than the a-plane lattice spacing of 0.3186 nm. The smooth surfaces produced in this study enable possibilities for laser facets or for new device structures that require high quality surfaces for GaN regrowth.

I. INTRODUCTION

Numerous advanced GaN semiconductor devices aim to leverage vertical architectures to achieve state-of-the-art performance and for efficient use of on-chip real estate.[1] Many of these devices rely on high density plasma etching to access buried

epitaxial layers whether to form contacts, create gate electrodes, or to regrow doped layers. Unlike Si, GaN is difficult to wet etch;[2] therefore Cl-based plasma etching has been the preferred method of patterning GaN.[3] Because plasmas inherently contain energetic ions which bombard the etched surface, reducing plasma etch damage and minimizing surface roughness of the etched surfaces is critical to prevent device degradation[3] and create high quality surfaces for regrowth.[4–6] Smooth faceted vertical surfaces are also necessary for fabrication of laser diodes. Our prior work has shown that elevated substrate temperatures may play a vital role in improving etch quality for ultra-smooth deep etching of GaN in a Cl_2-Ar plasma. Pillars with faceted sidewalls as smooth as 1.24 nm root-mean-square roughness (R_q) have been etched in a PlasmaQuest Electron Cyclotron Resonance (ECR) high-density plasma etch system that lacked active temperature control but where samples experience temperatures up to 200 °C due to self-heating from plasma exposure.[7] The elevated temperatures were believed to be, in part, responsible for producing high quality etch characteristics such as nanometer-scale sidewall roughness, crystallographically faceted surfaces, and >20:1 etch selectivities. Temperature is not treated as a typical etch optimization parameter in the majority of GaN etch studies, although reports exist.[8–15] Etching is often performed near room temperature (~15-30 °C)[16–29] even though temperature is known to influence the surface reaction kinetics and the volatility and desorption of etch byproducts.[30,31] In this study, we treat temperature as an important variable in GaN etching to understand how it affects the etch rate, selectivity, and surface morphology. We report ultra-smooth GaN structures with subnanometer R_q obtained under various temperatures, ICP powers, and RF powers using an Oxford PlasmaPro 100.

II. EXPERIMENTAL

n-GaN epitaxial layers grown on c-plane sapphire substrates by metal-organic chemical vapor deposition (Semiconductor Wafer, Inc.) were used for these experiments. As received wafers were diced into coupons and cleaned in ultrasonic solvent baths and self-heated 3:1 H_2SO_4:H_2O_2. A Plasma-Therm plasma-enhanced chemical vapor deposition system was used to deposit 1.0 µm-thick SiO_2 masking layers on the cleaned (0001) epilayer surfaces. Depositions were performed at 320 °C using 400 sccm 2% SiH_4/N_2, 900 sccm N_2O, 40 W RF, and 0.12 kPa (900 mTorr). Arrays of 1-10 µm diameter circles were defined using standard photolithography. Pattern transfer into the SiO_2 layer was carried out by dry etching in a C_4F_8/Ar plasma. After mask patterning, photoresist and etch residues were removed in ultrasonic solvent baths followed by self-heated 3:1 H_2SO_4:H_2O_2. The samples were then descummed in an O_2 plasma for 15-20 min. The crystallographic orientation of the substrates was maintained throughout the processing by scribing the backside of each chip after die singulation.

Prior to each GaN etch, the etch chamber was cleaned using an O_2 plasma at $2.7x10^{-3}$ kPa (20 mTorr), 2000 W ICP power, 150 W RF power, and 100 sccm O_2. The chamber was then conditioned with a Cl_2-Ar plasma generated using the process parameters under investigation for the subsequent etch. After conditioning, samples were placed on a sapphire carrier wafer that was mechanically clamped to the lower electrode upon loading. Thermal grease was neglected as no product could be found that could withstand the full temperature range in this study. Sapphire was chosen as the carrier as it does not appreciably etch in the Cl_2-Ar plasma.[32] The Cl_2 and Ar gas flow rates were fixed at 28 sccm and 3.5 sccm, respectively. A process pressure of $2.7x10^{-4}$ kPa (2

mTorr) was used throughout this work. Cross-sectional scanning electron microscopy (SEM) was carried out using a ThermoFisher Apreo SEM to evaluate the micropillar etch rates, profile, and etched surface morphology. On select samples, tapping-mode atomic force microscopy (AFM) was performed using a Bruker Dimension Icon system at EAG Laboratories for high resolution imaging of the micropillar sidewall to quantify roughness. Mask etch rates were determined by spectroscopic reflectivity measurements using a Toho Technology TohoSpec 3100 on SiO_2-coated Si samples that were simultaneously exposed to the same plasma conditions as their companion GaN etch parts. Etch selectivity values were obtained from the ratio of the GaN-to-SiO_2 etch rates.

III. Results and Discussion

As plasma conditions are interconnected, the interplay between RF power which controls the ion energy bombarding the samples and temperature were investigated. Temperature is expected to play a larger role when the etch is more chemically dominated, i.e. when the ion energy is low. The RF power was varied from 5 W to 100 W at both 50 °C and 200 °C while holding the ICP power at 300 W. Figure 1(a) shows SEM images of micropillars etched in this series. At high RF power (i.e. 100 W), physical etching dominates, and the etch morphology appears most similar between the two temperatures. As RF power is decreased, the etch was found to become more chemical with sidewall faceting emerging at both substrate temperatures. This suggests that faceting is more sensitive to RF power than temperature. Etching revealed a-plane facets on convex sidewall surfaces and m-plane facets on concave surfaces, consistent with wet etching techniques[33] and dry etching of other hexagonal systems such as 4H- and 6H-SiC.[34] a-plane facets on convex surfaces indicate that the a-plane etches faster

than the m-plane.[33] Trenching was also reduced with decreased RF power, suggesting that fewer reflected ions are accumulating at lower RF powers, causing a reduction in localized etch rate near the micropillar base.[35] At RF powers of 75 W and lower, the effect of temperature on the sidewall surface morphology is evident. At 50 °C, vertical striations are formed on the pillars, and higher etch temperatures produced smoother sidewall surfaces with small amounts of lateral etching.

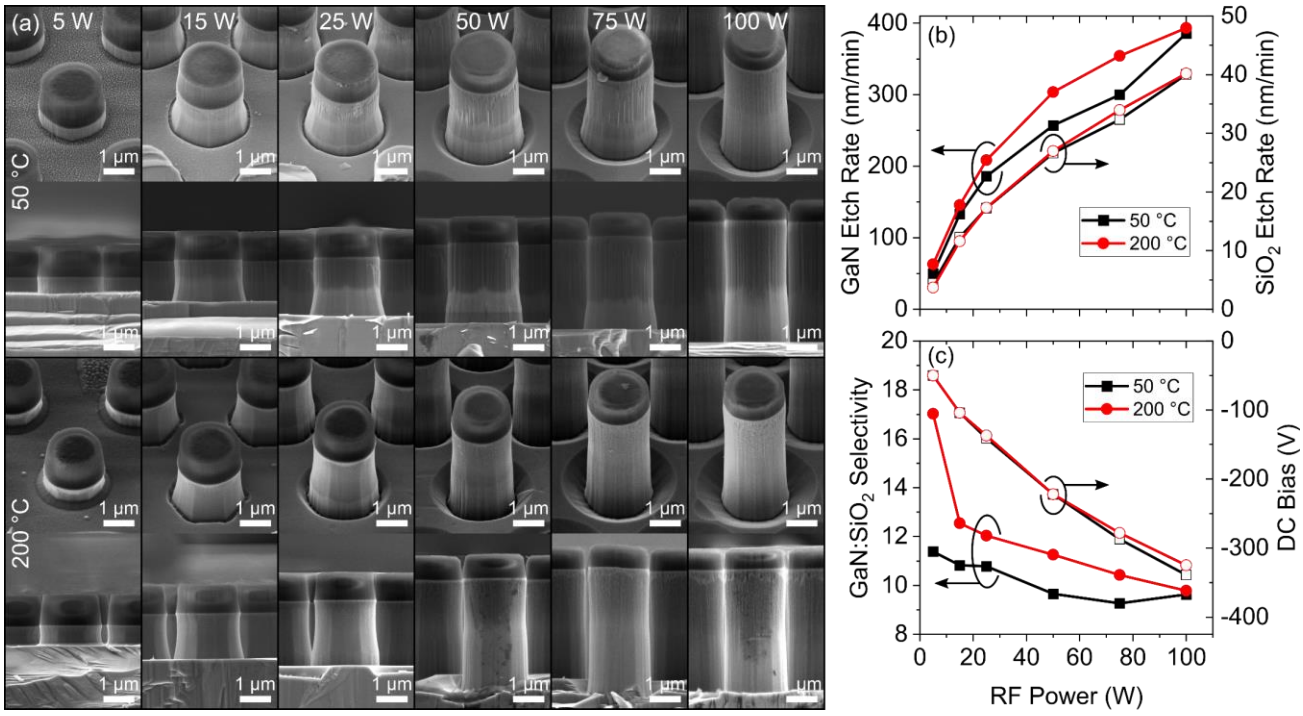

Figure 1. (a) Scanning electron images of GaN micropillars etched at 5-100 W RF power at both 50 °C and 200 °C. The ICP power was held at 300 W. Facets emerge at lower RF powers, and higher temperatures results in lower sidewall roughness. (b) GaN etch rate and SiO_2 etch rate as a function of RF power at 50 °C and 200 °C. (c) GaN:SiO_2 selectivity and DC bias as a function of the RF power at 50 °C and 200 °C.

AFM was used to quantify the roughness of the sidewalls of the pillars etched at 25 W RF power at both 50 °C and 200 °C. Figure 2 shows the AFM topographic images taken along the length of the micropillar sidewall surfaces. R_q for the 200 °C (1.99 nm)

sample was found to be 2.7 times smoother than at 50 °C etch (5.34 nm). R_q of the 200 °C sample is comparable to our prior report.[7] The vertical striations in the 50 °C sample are transferred from the edge of the SiO_2 mask. The features in the 200 °C sample do not have a directionality and are formed by a different mechanism.

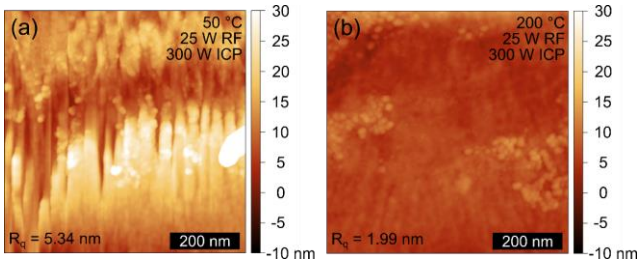

Figure 2. Atomic force micrographs of pillar sidewalls etched at 300 W ICP power, 25 W RF power, and at (a) 50 °C and (b) 200 °C. Increasing the substrate temperature reduces R_q from 5.34 nm to 1.99 nm.

Increased table temperature also led to increased etch rates and selectivity for this etch series, particularly at lower RF powers. As shown in Figure 1(b), the etch rate monotonically increases with RF power, and a maximum GaN etch rate of 0.4 μm/min was obtained at 200 °C. The etch rates at 50 °C and 200 °C and 100 W RF power nearly converge. This may indicate that the etch is in a more physically dominated regime where temperature plays a less important role or that higher ion bombardment energies are locally increasing the surface temperature and thus converging the etch conditions. The SiO_2 etch rates (Figure 1(b)) increased with increasing RF power but was not appreciably affected by increasing the temperature from 50 to 200 °C. The etch rate of SiO_2 in a Cl_2-Ar plasma is known to be limited by physical sputtering of O atoms from the surface and not strongly influenced by temperature.[36] As the RF power is lowered, the GaN:SiO_2 selectivity (Figure 1(c)) increases as the SiO_2 etch rate decreases more rapidly than the GaN. Etching at 200 °C increases the selectivity. A maximum selectivity of 17:1 GaN:

SiO_2 was obtained at 200 °C using 5 W RF power. The measured DC bias as a function of RF power is found in Figure 1(c).

Subsequent experiments were performed to shift the etch to a more highly chemically dominant regime by varying the ICP power from 300 W to 2000 W at both 50 °C and 200 °C. The increase in plasma density results in more radicals available in the plasma for chemical etching. The RF power was held at 25 W. SEM images of the etch series are found in Figure 3(a). As the ICP power is increased, faceting becomes more prominent, and the amount of undercutting increases. The amount of trenching around the pillars is also strongly affected by the ICP power. The trench is narrowest at 300 W and then becomes increasingly wider as the power is increased. At 1500 W, small "trenches" exist only where the vertices of the pillar facets meet the floor, and at 2000 W, the trenches disappear. We propose that the widening and eventual elimination of the trench is a result of increased lateral etching relative to vertical etching on the floor. As the in-plane etching of the crystal increases relative to the out-of-plane etching, any nonhorizontal surfaces will etch away. The overall effect is that depressions in the floor will become wider while protrusions will become narrower and eventually eliminated. This hypothesis is further supported by the decreasing DC bias with increasing ICP power (Figure 3(c)) which results in a more chemical etch. The above hypothesis neglects the etch rates of any defects present in the underlying GaN, which may be expected to etch even faster than in-plane etching. This can be observed by the increasingly higher density of pits on the GaN floor at higher ICP powers which are presumably threading dislocations which selectively etch more quickly.[37,38]

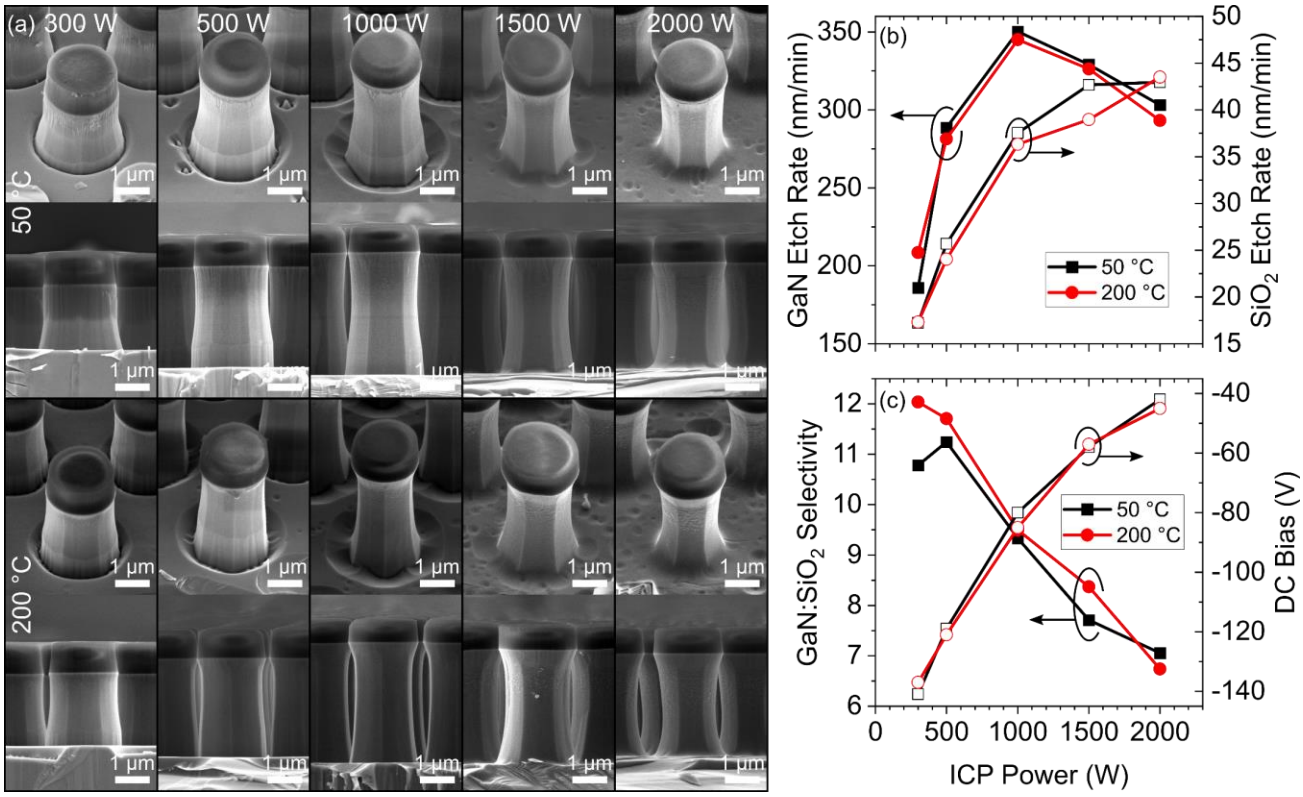

Figure 3. (a) Scanning electron images of GaN micropillars etched at 300-2000 W ICP at both 50 °C and 200 °C. The RF power was held at 25 W. Lateral etching increases and trenching decreases with the ICP power due to enhanced chemical etching. (b) GaN etch rate and SiO_2 etch rate as a function of the ICP power at 50 °C and 200 °C. (c) GaN:SiO_2 selectivity and DC bias as a function of the ICP power at 50 °C and 200 °C.

Competing effects influence the GaN etch rate as the ICP power is increased (Figure 3(b)). The etch rate rapidly increases from ~0.2 μm/min at 300 W to ~0.35 μm/min at 1000 W despite the DC bias decreasing from ~-140 V to ~-85V over the same ICP power range. The increased etch rate is due to higher ion and/or radical flux to the sample surface. As the ICP is further increased to 1500 W and then 2000 W, the etch rate decreases to ~0.30 μm/min presumably due to the decreasing ion energy at lower DC biases. Thus, there may be a rate limiting etch barrier that requires a threshold ion energy

in the range of ~-85 eV, consistent with Ohba, et al.[39] who found that a self-limiting etch regime exists at 50-100 V of DC bias during atomic layer etching of GaN in a Cl_2-Ar plasma. Table temperature does not strongly affect the GaN etch rate in this series. This suggests that surface reaction kinetics are not rate limiting along the c-face or that increased ICP power causes the local surface temperature to increase above 50 °C. The SiO_2 etch rate (Figure 3(b)) increases over the whole range of ICP powers and is not strongly influenced by temperature. This suggests that the SiO_2 etch rate is limited by ion flux to the mask surface under these conditions; however, the etch rate flattens out at lower DC biases possibly indicating that an ion energy threshold is located near ~-45V, consistent with prior reports.[36] The decreasing GaN:SiO_2 selectivity (Figure 3(c)) with ICP power indicates that plasma density plays a larger role in SiO_2 etching than in GaN etching under these conditions.

To further explore the effect of temperature on the GaN etching, an expanded temperature series from 50 to 400 °C at 25 W and 75 W RF was performed. An ICP power of 1000 W was down-selected based on the high GaN etch rate, smooth sidewalls, and moderate lateral etching. SEM images of the etched pillars can be found in Figure 4(a). Increasingly more lateral etching is observed at higher temperatures for both the pillar sidewall and the floor. The higher lateral etching of the pillars indicates that the etch is chemically driven and that temperature has a strong influence on the etch morphology. Under 25 W RF power, the pillars are hexagonally faceted with facets parallel to the a-plane under each temperature; however, at 75 W RF power, the pillars shift from hexagonal faceting at 50 °C to 12-sided faceting as the temperatures is increased. The 12-facets are composed of 6 facets parallel to each of the a- and m-planes.

At higher temperatures, the etch rates of the a- and m-planes may begin to converge such that facets of each plane emerge. The trenching at the floor of the pillars is also strongly influence by the etch temperature. The trenches are prominent at lower temperatures and widen out and fade away as the temperature increases. At 400 °C, trenching is eliminated. A similar explanation can be made here as was made for the ICP power series. As the etch becomes more chemically driven (in this case by temperature), the lateral etch rates increase relative to the c-plane etch rate. The high in-plane etch rate smooths the floor surface by expanding depressions and shrinking protrusions. At 25 W RF power, pitting on the floor emerges due to a more defect selective etch. When the RF power is increased to 75 W, the pitting is drastically reduced because of the enhanced etch rate in the c-direction. At 75 W RF power, the SiO_2 mask clearly erodes, particularly around the edges. This results in sidewall roughness around the top of the pillar. The lateral etching of the mask at 400 °C is so great that GaN at the top of the pillar is etched away.

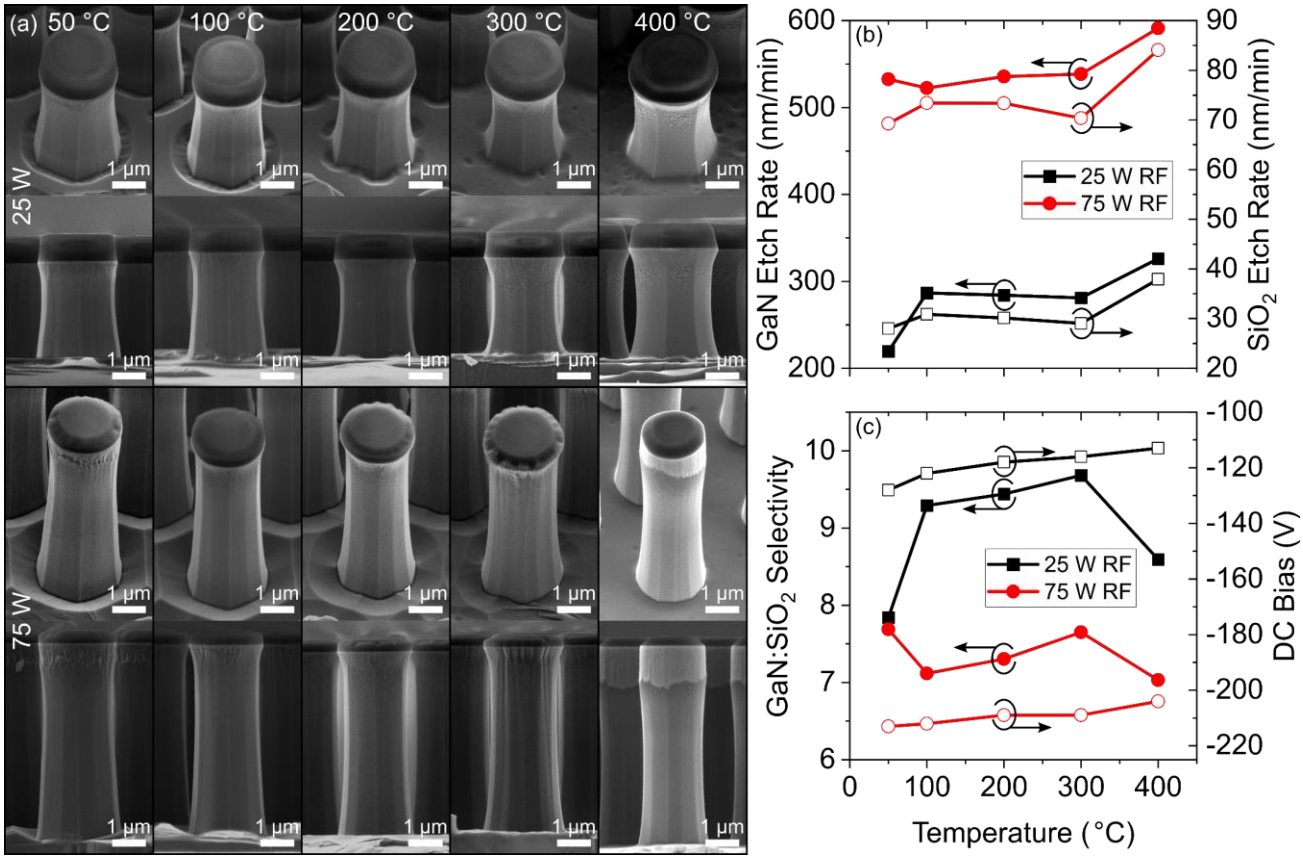

Figure 4. (a) Scanning electron images of GaN micropillars etched at 50-400 °C at 25 W and 75 W RF power. The ICP power was held at 1000 W. Lateral etching increases and trenching decreases with the temperature due to enhancement of chemical etching. (b) GaN etch rate and SiO_2 etch rate as a function of the substrate temperature at 25 W and 75 W RF power. (c) GaN:SiO_2 selectivity and DC bias as a function of the substrate temperature at 25 W and 75 W RF power.

The etches at all conditions appear smooth, and AFM topographs (Figure 5) of pillar sidewalls were taken for the samples etched at 50 °C, 200 °C, and 400 °C and 25 W RF power. Each etch was found to be extremely smooth, with R_q <0.50 nm, which is a significant reduction in roughness compared to our prior ECR work (R_q = 1.34 nm).[7] The 50 °C etch was found to be the smoothest, with an R_q of 0.20 nm, comparable to epi-ready surfaces and as-grown GaN. A slight increase in roughness was observed with increased temperature, which is distinct from the first RF power series performed under a

more intermediate chemical/physical etch regime where temperature leads to a decrease in R_q. The increased roughness and bumpy surface morphology for the temperature may be a direct consequence of increased isotropy at higher temperatures or micromasking of the sidewalls couple with a higher tendency to etch laterally. The origin of these features warrants further investigation so that they can be controlled. These results suggest that the effect of temperature on the sidewall roughness and etch characteristics is highly dependent on the etch regime and due to the interdependent nature of etch parameters in plasma etching.

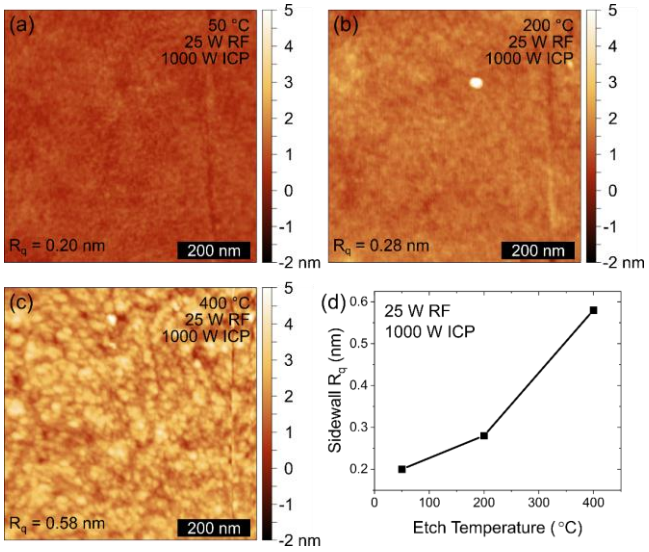

Figure 5. Atomic force micrographs of pillar sidewalls etched at (a) 50, (b) 200, and (c) 400 °C with an RF power of 25 W and ICP power of 1000 W. A plot of the roughness is shown in (d). As the temperature is increased, the sidewall roughness, R_q, increases.

The vertical GaN etch rate (see Figure 4(b)) remains relatively flat for a given RF power across the temperature range with the etch rate lower at 50 °C and higher at 400 °C. This modest effect of temperature on the vertical GaN etch rate suggests that the rate limiting step is governed by a physical process. The SiO_2 etch rate (Figure 4(b)) also

remains relatively flat across the temperature range, consistent with it being rate limited by sputtering of O. The GaN:SiO_2 selectivity (Figure 4(c)) does not vary much with temperature but is increased as the RF power is decreased. The DC bias in the etcher is not strongly influenced by the table temperature (Figure 4(c)).

IV. SUMMARY AND CONCLUSIONS

The role of substrate temperature in influencing the etch characteristics was found to be highly etch regime dependent. Temperature was shown to improve the sidewall etch morphology in an intermediate physical/chemical etch regime, at low-moderate RF powers (reduced physical bombardment) and low ICP powers (lower plasma densities). The sidewall roughness was not affected by temperature under strongly physically dominant etch conditions, at low ICP powers and high RF powers. Under highly chemically dominant etch conditions (low RF power, high ICP power), extremely smooth sidewalls with <0.5 nm roughness were achieved with temperature leading to slight increases in roughness. The results presented here show how smooth etched GaN surface can be produced which can potentially create better surfaces for GaN epitaxial regrowth or laser diode fabrication. In future work, more optimizations can still be done to further improve the etch characteristics to decrease undercutting, trenching, etc.

ACKNOWLEDGMENTS

This work was performed under the auspices of the U.S. Department of Energy by Lawrence Livermore National Laboratory under Contract DE-AC52-07NA27344, LDRD Tracking #19-FS-005, LLNL-JRNL-822768.

References

[1] H. Amano, Y. Baines, E. Beam, M. Borga, T. Bouchet, P.R. Chalker, M. Charles, K.J. Chen, N. Chowdhury, R. Chu, C.D. Santi, M.M.D. Souza, S. Decoutere, L.D. Cioccio, B. Eckardt, T. Egawa, P. Fay, J.J. Freedsman, L. Guido, O. Häberlen, G. Haynes, T. Heckel, D. Hemakumara, P. Houston, J. Hu, M. Hua, Q. Huang, A. Huang, S. Jiang, H. Kawai, D. Kinzer, M. Kuball, A. Kumar, K.B. Lee, X. Li, D. Marcon, M. März, R. McCarthy, G. Meneghesso, M. Meneghini, E. Morvan, A. Nakajima, E.M.S. Narayanan, S. Oliver, T. Palacios, D. Piedra, M. Plissonnier, R. Reddy, M. Sun, I. Thayne, A. Torres, N. Trivellin, V. Unni, M.J. Uren, M.V. Hove, D.J. Wallis, J. Wang, J. Xie, S. Yagi, S. Yang, C. Youtsey, R. Yu, E. Zanoni, S. Zeltner, Y. Zhang, The 2018 GaN power electronics roadmap, J. Phys. D: Appl. Phys. 51 (2018) 163001. https://doi.org/10.1088/1361-6463/aaaf9d.

[2] D. Zhuang, J.H. Edgar, Wet etching of GaN, AlN, and SiC: a review, Materials Science and Engineering: R: Reports. 48 (2005) 1–46. https://doi.org/10.1016/j.mser.2004.11.002.

[3] S.J. Pearton, E.A. Douglas, R.J. Shul, F. Ren, Plasma etching of wide bandgap and ultrawide bandgap semiconductors, Journal of Vacuum Science & Technology A. 38 (2020) 020802. https://doi.org/10.1116/1.5131343.

[4] K. Fu, H. Fu, X. Huang, H. Chen, T.-H. Yang, J. Montes, C. Yang, J. Zhou, Y. Zhao, Demonstration of 1.27 kV Etch-Then-Regrow GaN p-n Junctions With Low Leakage for GaN Power Electronics, IEEE Electron Device Letters. 40 (2019) 1728–1731. https://doi.org/10.1109/LED.2019.2941830.

[5] G.W. Pickrell, A.M. Armstrong, A.A. Allerman, M.H. Crawford, C.E. Glaser, J. Kempisty, V.M. Abate, Investigation of dry-etch-induced defects in >600 V regrown, vertical, GaN, p-n diodes using deep-level optical spectroscopy, Journal of Applied Physics. 126 (2019) 145703. https://doi.org/10.1063/1.5110521.

[6] K. Zhang, T. Takahashi, D. Ohori, G. Cong, K. Endo, N. Kumagai, S. Samukawa, M. Shimizu, X. Wang, High-quality nanodisk of InGaN/GaN MQWs fabricated by neutral-beam-etching and GaN regrowth: towards directional micro-LED in top-down structure, Semicond. Sci. Technol. 35 (2020) 075001. https://doi.org/10.1088/1361-6641/ab8539.

[7] S.E. Harrison, L.F. Voss, A.M. Torres, C.D. Frye, Q. Shao, R.J. Nikolić, Ultradeep electron cyclotron resonance plasma etching of GaN, Journal of Vacuum Science & Technology A. 35 (2017) 061303. https://doi.org/10.1116/1.4994829.

[8] R. Debnath, J.-Y. Ha, B. Wen, D. Paramanik, A. Motayed, M.R. King, A.V. Davydov, Top-down fabrication of large-area GaN micro- and nanopillars, Journal of Vacuum Science & Technology B. 32 (2014) 021204. https://doi.org/10.1116/1.4865908.

[9] Z. Liu, J. Pan, T. Kako, K. Ishikawa, K. Takeda, H. Kondo, O. Oda, M. Sekine, M. Hori, Suppression of plasma-induced damage on GaN etched by a Cl2 plasma at high temperatures, Jpn. J. Appl. Phys. 54 (2015) 06GB04. https://doi.org/10.7567/JJAP.54.06GB04.

[10] Z. Liu, J. Pan, A. Asano, K. Ishikawa, K. Takeda, H. Kondo, O. Oda, M. Sekine, M. Hori, Investigation of effects of ion energies on both plasma-induced damage and surface morphologies and optimization of high-temperature Cl2 plasma etching of GaN, Jpn. J. Appl. Phys. 56 (2017) 026502. https://doi.org/10.7567/JJAP.56.026502.

[11] Z. Liu, A. Asano, M. Imamura, K. Ishikawa, K. Takeda, H. Kondo, O. Oda, M. Sekine, M. Hori, Thermally enhanced formation of photon-induced damage on GaN films in Cl2 plasma, Jpn. J. Appl. Phys. 56 (2017) 096501. https://doi.org/10.7567/JJAP.56.096501.
[12] Z. Liu, K. Ishikawa, M. Imamura, T. Tsutsumi, H. Kondo, O. Oda, M. Sekine, M. Hori, Temperature dependence on plasma-induced damage and chemical reactions in GaN etching processes using chlorine plasma, Jpn. J. Appl. Phys. 57 (2018) 06JD01. https://doi.org/10.7567/JJAP.57.06JD01.
[13] A. Tanide, S. Nakamura, A. Horikoshi, S. Takatsuji, M. Kohno, K. Kinose, S. Nadahara, K. Ishikawa, M. Sekine, M. Hori, Effects of BCl3 addition to Cl2 gas on etching characteristics of GaN at high temperature, Journal of Vacuum Science & Technology B. 37 (2019) 021209. https://doi.org/10.1116/1.5082345.
[14] T. Kako, Z. Liu, K. Ishikawa, H. Kondo, O. Oda, M. Sekine, M. Hori, Elevated-temperature etching of gallium nitride (GaN) in dual-frequency capacitively coupled plasma of CH4/H2 at 300–500 °C, Vacuum. 156 (2018) 219–223. https://doi.org/10.1016/j.vacuum.2018.07.040.
[15] A.P. Shah, A. Azizur Rahman, A. Bhattacharya, Temperature-dependence of Cl2/Ar ICP-RIE of polar, semipolar, and nonpolar GaN and AlN following BCl3/Ar breakthrough plasma, Journal of Vacuum Science & Technology A. 38 (2019) 013001. https://doi.org/10.1116/1.5123787.
[16] R.J. Shul, C.G. Willison, M.M. Bridges, J. Han, J.W. Lee, S.J. Pearton, C.R. Abernathy, J.D. MacKenzie, S.M. Donovan, High-density plasma etch selectivity for the III–V nitrides, Solid-State Electronics. 42 (1998) 2269–2276. https://doi.org/10.1016/S0038-1101(98)00224-X.
[17] R.J. Shul, G.B. McClellan, S.A. Casalnuovo, D.J. Rieger, S.J. Pearton, C. Constantine, C. Barratt, R.F. Karlicek, C. Tran, M. Schurman, Inductively coupled plasma etching of GaN, Appl. Phys. Lett. 69 (1996) 1119–1121. https://doi.org/10.1063/1.117077.
[18] B. Rong, E. van der Drift, R.J. Reeves, W.G. Sloof, R. Cheung, Inductively coupled plasma etching of GaN and its effect on electrical characteristics, Journal of Vacuum Science & Technology B: Microelectronics and Nanometer Structures Processing, Measurement, and Phenomena. 19 (2001) 2917–2920. https://doi.org/10.1116/1.1421543.
[19] S. Tripathy, A. Ramam, S.J. Chua, J.S. Pan, A. Huan, Characterization of inductively coupled plasma etched surface of GaN using Cl2/BCl3 chemistry, Journal of Vacuum Science & Technology A. 19 (2001) 2522–2532. https://doi.org/10.1116/1.1392400.
[20] Y.-J. Han, S. Xue, W.-P. Guo, C.-Z. Sun, Z.-B. Hao, Y. Luo, Characteristics of n-GaN After Cl2/Ar and Cl2/N2 Inductively Coupled Plasma Etching, Jpn. J. Appl. Phys. 42 (2003) 6409. https://doi.org/10.1143/JJAP.42.6409.
[21] S. Zhou, B. Cao, S. Liu, Dry etching characteristics of GaN using Cl2/BCl3 inductively coupled plasmas, Applied Surface Science. 257 (2010) 905–910. https://doi.org/10.1016/j.apsusc.2010.07.088.
[22] J. Ladroue, A. Meritan, M. Boufnichel, P. Lefaucheux, P. Ranson, R. Dussart, Deep GaN etching by inductively coupled plasma and induced surface defects, Journal of

Vacuum Science & Technology A. 28 (2010) 1226–1233. https://doi.org/10.1116/1.3478674.
[23] A. Baharin, R.S. Pinto, U.K. Mishra, B.D. Nener, G. Parish, Low resistivity contacts to plasma etched Mg-doped GaN using very low power inductively coupled plasma etching, Thin Solid Films. 519 (2011) 3686–3689. https://doi.org/10.1016/j.tsf.2011.01.276.
[24] D.S. Rawal, H. Arora, V.R. Agarwal, A. Kapoor, S. Vinayak, B.K. Sehgal, R. Muralidharan, D. Saha, H.K. Malik, Cl2/Ar based Inductively Coupled Plasma Etching of GaN/AlGaN Structure, in: 16th International Workshop on Physics of Semiconductor Devices, International Society for Optics and Photonics, 2012: p. 85490L. https://doi.org/10.1117/12.925529.
[25] D.S. Rawal, H.K. Malik, V.R. Agarwal, A.K. Kapoor, B.K. Sehgal, R. Muralidharan, $\hboxBCl_3/\hboxCl_2$-Based Inductively Coupled Plasma Etching of GaN/AlGaN Using Photoresist Mask, IEEE Transactions on Plasma Science. 40 (2012) 2211–2220. https://doi.org/10.1109/TPS.2012.2206831.
[26] D.S. Rawal, B.K. Sehgal, R. Muralidharan, H.K. Malik, A. Dasgupta, Effect of BCl3 concentration and process pressure on the GaN mesa sidewalls in BCl3/Cl2 based inductively coupled plasma etching, Vacuum. 86 (2012) 1844–1849. https://doi.org/10.1016/j.vacuum.2012.04.018.
[27] D.S. Rawal, H. Arora, V.R. Agarwal, S. Vinayak, A. Kapoor, B.K. Sehgal, R. Muralidharan, D. Saha, H.K. Malik, GaN etch rate and surface roughness evolution in Cl2/Ar based inductively coupled plasma etching, Thin Solid Films. 520 (2012) 7212–7218. https://doi.org/10.1016/j.tsf.2012.07.117.
[28] Z. Liu, Y. Wang, X. Xia, H. Yang, J. Li, C. Gu, Fabrication of GaN hexagonal cones by inductively coupled plasma reactive ion etching, Journal of Vacuum Science & Technology B. 34 (2016) 041226. https://doi.org/10.1116/1.4954986.
[29] X. Li, P. Ma, X. Ji, T. Wei, X. Tan, J. Wang, J. Li, Implementation of slow and smooth etching of GaN by inductively coupled plasma, J. Semicond. 39 (2018) 113002. https://doi.org/10.1088/1674-4926/39/11/113002.
[30] S.J. Pearton, J.C. Zolper, R.J. Shul, F. Ren, GaN: Processing, defects, and devices, Journal of Applied Physics. 86 (1999) 1–78. https://doi.org/10.1063/1.371145.
[31] N. Okamoto, A. Takahashi, Y. Minoura, Y. Kumazaki, S. Ozaki, T. Ohki, N. Hara, K. Watanabe, Deep GaN through-substrate via etching using Cl2/BCl3 inductively coupled plasma, Journal of Vacuum Science & Technology A. 38 (2020) 063003. https://doi.org/10.1116/6.0000526.
[32] C.D. Frye, S.B. Donald, C.E. Reinhardt, R.J. Nikolic, L.F. Voss, S.E. Harrison, Ultrahigh GaN:SiO2 etch selectivity by in situ surface modification of SiO2 in a Cl2-Ar plasma, Materials Research Letters. 9 (2021) 105–111. https://doi.org/10.1080/21663831.2020.1847735.
[33] B. Leung, M.-C. Tsai, G. Balakrishnan, C. Li, S.R.J. Brueck, J.J. Figiel, P. Lu, G.T. Wang, Highly Anisotropic Crystallographic Etching for Fabrication of High-Aspect Ratio GaN Nanostructures, San Diego. (2016) 45.
[34] C.D. Frye, D. Funaro, A.M. Conway, D.L. Hall, P.V. Grivickas, M. Bora, L.F. Voss, High temperature isotropic and anisotropic etching of silicon carbide using forming gas, Journal of Vacuum Science & Technology A. 39 (2021) 013203. https://doi.org/10.1116/6.0000533.

[35] S.V. Nguyen, D. Dobuzinsky, S.R. Stiffler, G. Chrisman, Substrate Trenching Mechanism during Plasma and Magnetically Enhanced Polysilicon Etching, J. Electrochem. Soc. 138 (1991) 1112. https://doi.org/10.1149/1.2085726.
[36] J.P. Chang, H.H. Sawin, Molecular-beam study of the plasma-surface kinetics of silicon dioxide and photoresist etching with chlorine, Journal of Vacuum Science & Technology B: Microelectronics and Nanometer Structures Processing, Measurement, and Phenomena. 19 (2001) 1319–1327. https://doi.org/10.1116/1.1387452.
[37] H.W. Choi, C. Liu, M.G. Cheong, J. Zhang, S.J. Chua, Exposure of defects in GaN by plasma etching, Appl. Phys. A. 80 (2005) 405–407. https://doi.org/10.1007/s00339-003-2372-5.
[38] A. Pandey, B.S. Yadav, D.S. Rao, D. Kaur, A.K. Kapoor, Dislocation density investigation on MOCVD-grown GaN epitaxial layers using wet and dry defect selective etching, Applied Physics A. 122 (2016) 614.
[39] T. Ohba, W. Yang, S. Tan, K.J. Kanarik, K. Nojiri, Atomic layer etching of GaN and AlGaN using directional plasma-enhanced approach, Jpn. J. Appl. Phys. 56 (2017) 06HB06. https://doi.org/10.7567/JJAP.56.06HB06.